GAVIN PUBLISHERS

Archives of Environmental Sciences and Environmental Toxicology

OPEN ACCESS

Gao Y, et al. Arch Environ Sci Environ Toxicol 4: 131.
DOI: 10.29011/2688-948X.100131

Research Article

Investigating and Analyzing the Water-Inrush Source at the Heading-Face of Coal Mines: A Case Study of Beixinyao Coal Mine in Shanxi Province, China

Yuping Gao[1,2], Jinyu Gao[2], Yuehong Cheng[3], Jianhua Yue[1*], Min Wang[2], Yuanzhi Zhang[4,5]

[1]China University of Mining and Technology, School of Resources and Geoscience, Xuzhou 221116, Jiangsu Province, China

[2]Datong Coal Mine Group Co. Ltd., Datong 037003, Shanxi Province, China

[3]China National Offshore Oil Corporation, Beijing 100010, China

[4]Nanjing University of Information Science and Technology, School of Marine Science, Nanjing 210044, China

[5]Chinese University of Hong Kong, Faculty of Social Science and Institute of Asia Pacific Studies, Hong Kong

[*]**Correspondence:** Jianhua Yue, China University of Mining and Technology, School of Resources and Geoscience, Xuzhou 221116, Jiangsu Province, China

Citation: Gao Y, Gao J, Cheng Y, Yue J, Wang M, et al. (2021) Investigating and Analyzing the Water-Inrush Source at the Heading-Face of Coal Mines: A Case Study of Beixinyao Coal Mine in Shanxi Province, China. Arch Environ Sci Environ Toxicol 4: 131. DOI: 10.29011/2688-948X.100131

Received Date: 26 January 2021; **Accepted Date:** February 09, 2021; **Published Date:** February 15, 2021

Abstract

This study investigated the water-inrush source of mining underground water via a case study of Beixinyao Coal Mine in Datong, Shanxi Province, China. The study mainly analyzed the impact factors for water inrush from the coalmine wells of the water outlet and the geological structure in the minefield, as well as changes in the roadway coal, rock formations, hydrographic data, water quality data, and C14 isotope analysis of water samples, trace element measurements, combined with underground verification. The kilometer grouting drilling data of the construction indicates that the source of water inrush is tectonic water and provides accurate data for the following steps of scientific engineering treatments. Field work with sampling collection allows data analysis based on laboratory testing to investigate sources of underground water-inrush in coal mines and accurately determine causes of water outflow in mining wells having water gushing, allowing timely formulation of corresponding measures, effective control of water damage, and finally, in the case of Beixinyao Coal Mine, assurance of safe production. This study can also provide a reference for similar coalmines in China or other countries.

Keywords: Coalmine groundwater; Coal fields; Water inrush; Coalmine heading-face

Introduction

Beixinyao Coal Mine is a new coalmine of Tongmei Group, located at the northern end of Ningwu Coalfield and southeast of the Shuonan Mining Area [1]. It has widths of 11.09 km from east to west and 12.59 km from north to south, for an area of 53.29 km^2, and has a production capacity of 400 Mt/a [2,3]. Due to tectonic developments, its geological and hydrogeological conditions are complicated, and water damage from the top and bottom aquifers poses a threat to coal seam mining (Figure 1). Significant hydrogeological exploration has been undertaken, along with investigation of the hydrogeological conditions in which the mine is located and between the major aquifers [4]. The aquifer's hydraulic connection and lithology, thickness, and water resistance still need to be investigated and assessed. Objective evaluation shows that the mine is susceptible to water inrush backplane from Ordovician limestone water [5]. Sedimentary strata in the mining field, from old to new, include the Ordovician Middle and Upper Majiagou Formations (O2s + x), the Carboniferous Benxi Formation (C2b), the Upper Taiyuan Formation (C3t), the Permian Shanxi Formation (P1s), a lower stone box group (P1x), an upper stone box group (P2s), a middle and upper update system of the fourth system (Q2 + 3), and a new system (Q4). The aquifer in the well field, from new to old, is divided into quaternary loose layer pore aquifer, upper and lower Shihezi Formation and Shiqianfeng Formation bottom sandstone fracture aquifer, Shanxi formation sandstone fracture aquifer, Taiyuan sandstone fracture aquifer, and limestone karst-fractured aquifer in the Upper Ordovician Middle Majiagou Formation [6].

During excavation of the return wing lane of the south wing system from north to south, a sudden gush of water appeared on the palm surface and gushing water volume gradually increased

to 316 m^3/h, then stayed steady at 300 m^3/h. During excavation of the south wing auxiliary transportation lane from north to south, water inrush also occurred on the floor and gushing water volume reached 300 m^3/h, after which the water volume stayed steady at 215 m3/h. To effectively control water damage in a timely manner, the source of water inrush needs to be identified [7-9].

This article comprehensively analyzes the reasons for water inrush from the area of the water outlet and the structure of coalmine fields, as well as changes in the roadway coal, rock formations, hydrographic and water quality data [10-12]. C^{14} isotope analysis of water samples, trace element measurements, combined with underground verification. The kilometer grouting drilling data of the construction indicates that the source of water inrush is tectonic water and provides accurate data for the next steps of scientific and engineering treatments.

Materials and Methods

Beixinyao Minefield Regional Structure

Beixinyao coalfield is located in the north of the Ningwu coalfield (Figure 1). Based on analysis of regional remote sensing data, the regional structural location is northwest of the Ningwu-Jingle syncline, which shows a north-northeast long axis distribution; the strata at the edges of the east and west wings have large inclination angles of up to 40-80° and some are even upside-down. The internal structure of the basin is unevenly developed, with the north more complex in the Ningwu-Yangfangkou area [8,9]. A series of large-scale near west or northeast east eastward tensile faults were developed, including the Wangwanzhuang fault, Dingjialiang fault, and Ningwu fault. Accompanied by secondary folds, such as the Wang Wan Zhuang fault spanning the east and west of the minefield, a series of large-scale north south extensional faults, such as the Motioning fault zone, are divided into two parts: The tectonic structure is the western boundary of the Shuonan Coalfield, and the Mayi fault is the eastern boundary of the Shuonan Coalfield, along with a series of northwestward nappe structures, the Anziping-Shihuling fault.

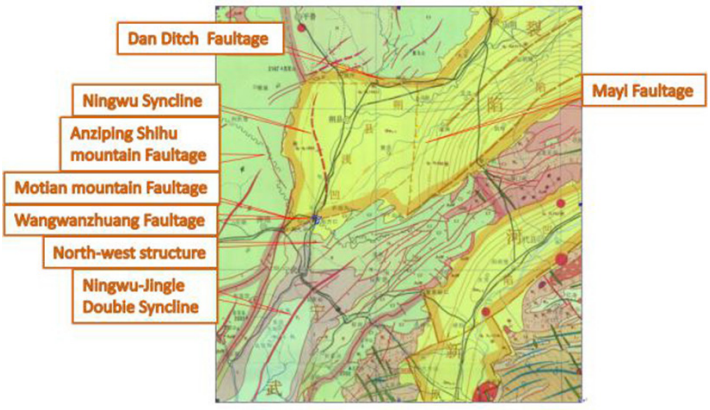

Figure 1: Structural outline of Beixinyao area.

Wellfield Structure

Affected by regional structure, faults and folds developed in the coal well field. The stratum as a whole runs northeast, leaning southeast or northwest, with an inclination angle of 4°-25°. There are 26 normal faults in the field, including nine faults exceeding 100 meters (Figure 2).

In the Beixinyao minefield, the topography is generally high on the east and west sides and low in the middle. Ordovician limestone is exposed on both the east and the west sides, and the area is large, directly supplying the Ordovician limestone formation. Groundwater runoff is generally from south to north and from west to east.

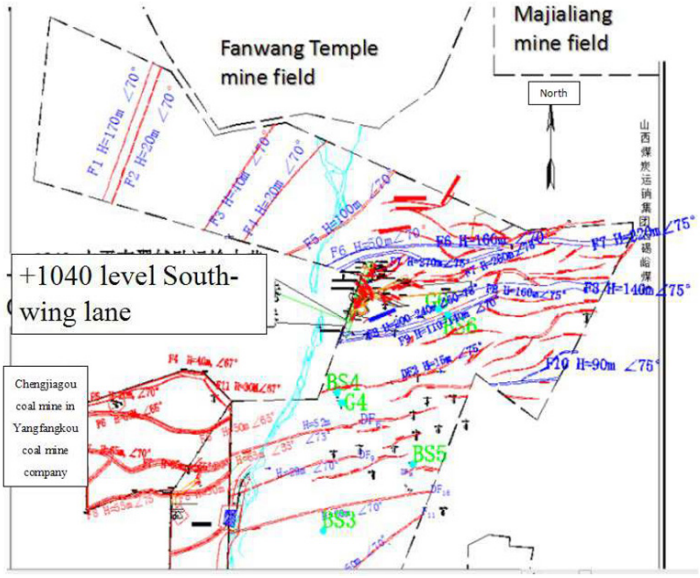

Figure 2: Structural outline of Beixinyao minefield.

From the perspective of the regional structure and the geological structure in the well field, a large nappe structure was formed in a northwestward direction. Early compression caused the formation to be inverted on the right side, with the limestone rising, and later stretching, forming a limestone collapse zone. This shows that the three lanes are located on the east flank of the north south structure, cutting the northwest trending nappe and tension structure, while meeting the northeast direction structure.

Identification of Water Source of Water Inrush Points

Structural Analysis of Water Inrush Points

The water outlet is located in the east of the north-south structure (i.e., the Huihe channel) in the north of the minefield (Figure 3). There are two east-west faults: F7, the Wangwanzhuang fault in the regional structure and the other in the middle of the F8 cutting block, the northwestward thrusting structure in the southern limestone fracture zone.

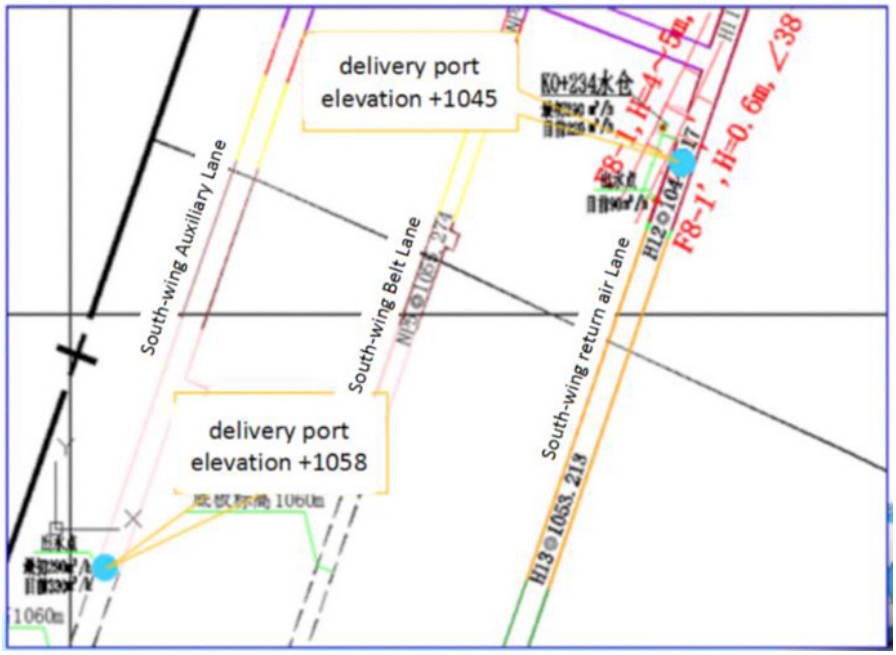

Figure 3: Plan view of outlet water point.

Left Wing of South Wing Auxiliary Transport Lane

Figure 4 shows a cross-sectional view of the left gangway drainage ditch of the south wing auxiliary transportation lane. It can be seen that the south wing auxiliary transportation lane is severely squeezed on both sides and is almost upright, which indicates that the stratum near the water outlet is squeezed by external forces, even as the stratum in the south stretches to form a limestone breccia fracture zone.

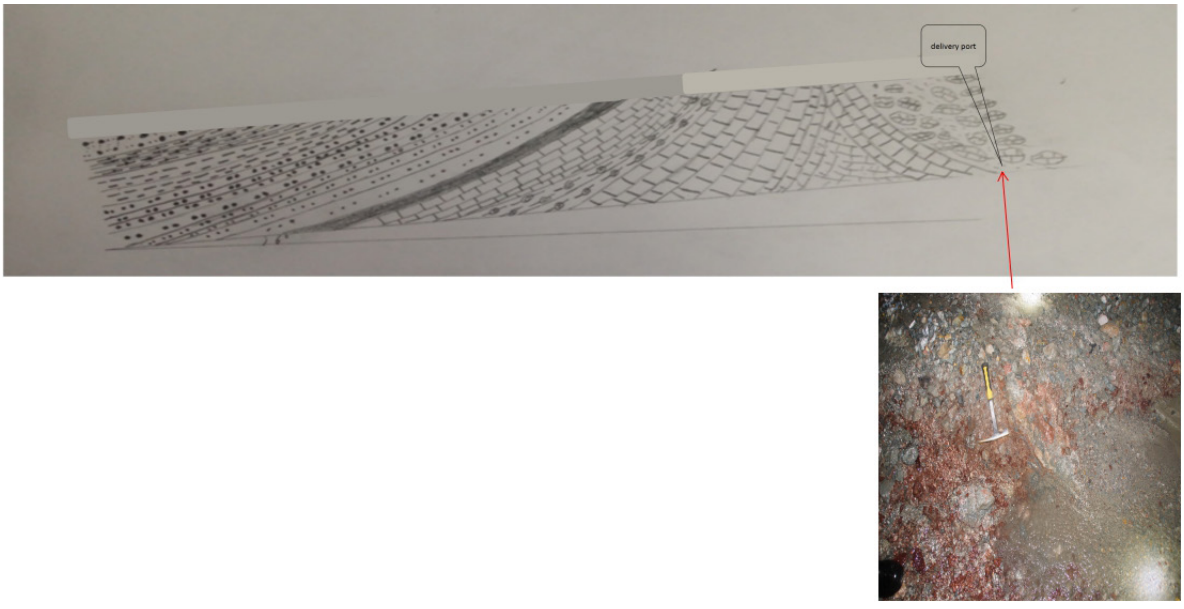

Figure 4: Sectional view of the left gangway of the South Wing Auxiliary Transport Lane (N-S →).

Water Sample for Water Chemical Laboratory Analysis

The following is a statistical table of water quality types of water outlets and nearby boreholes (Table 1):

No.	Location	K+Na (%)	Ca (%)	Mg (%)	CI (%)	SO_4 (%)	HCO_3 (%)
1	BS3	16.2	9.7	1.3	4.1	12.8	55.9
2	BS4	7.5	15.9	2.6	2.9	9.3	61.8
3	BS5	6.6	14.8	4.0	2.2	20.7	51.7
4	BS6	12.7	9.5	3.9	2.5	20.4	51.0
5	G4	13.8	9.0	2.9	2.8	8.2	63.3
6	G6	24.7	4.5	1.1	12.8	22.2	34.6
7	NHF	4.7	15.5	4.4	3.1	12.3	60.0
8	NFY	4.1	16.3	4.7	2.4	8.3	64.1
9	NPD	14.2	10.0	3.0	1.4	33.2	38.2

Table 1: Results of water quality analysis for samples from drilling and water outlets.

By processing the data, a piper three-line diagram is generated Figure 5:

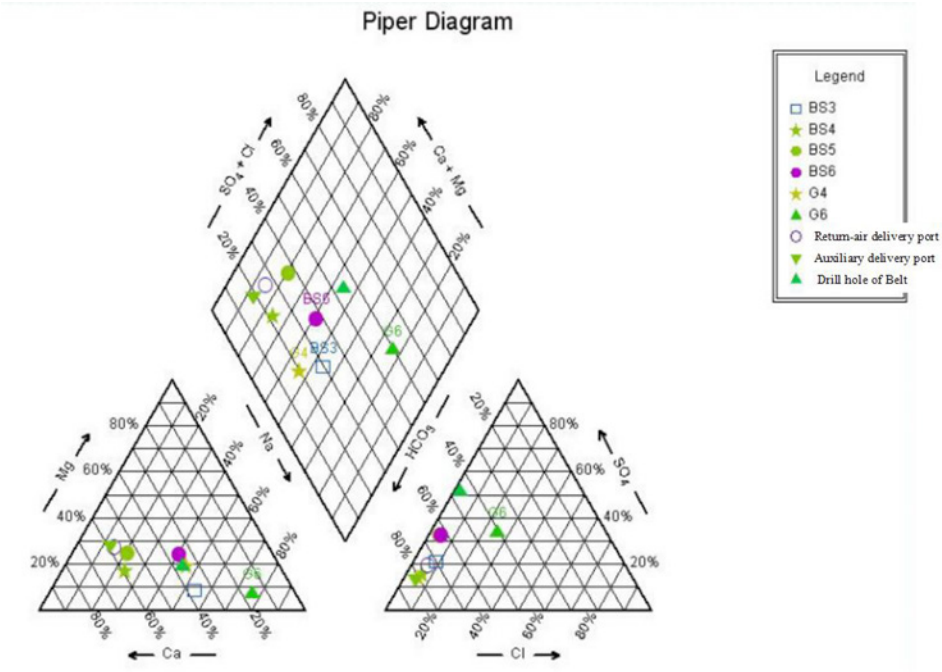

Figure 5: Three-line diagram of the piper for water quality analysis.

The piper chart shows that the water quality at the water outlet point differs from the water quality of the Taiyuan Formation and the Ordovician limestone water. At present, the water volume of the two outlet lanes is essentially stable and has not changed for nearly a month, indicating that the Taiyuan Formation and the Ordovician limestone water aquifer have lateral recharge for the water outlets of the excavated alleys. Based on the geological structure of the area and the flow direction of the runoff zone (southwest to northeast), the F8 fault is believed to conduct water from the Huihe River from north to south. The structure has a certain hydraulic connection.

Analysis of Water Quality Types of Hydrological Pores

It can be seen from the preceding figure that after the water gushing from each of the hydrological observation holes in the south wing alley, drilling water levels have different depths Table 2, with the Taiyuan Group G6 observation hole in the same hydrological unit having the greatest indicating that the water layer in the water point recharges the coal seam. The bottom sandstone aquifer is relatively large [13-15]. The water quality types of the South Wing Backwind Lane and the South Wing Auxiliary Transport Lane are both HCO_3—Ca · Mg, and the water volume at both water outlets is currently steady at 300 m³/h; both are characterized by mixed water.

Drilling	Layers	Water type	Initiate water level height (m)	Current water level height (m)	Water depth falling down（m）
BS3	O_{2S+X}	HCO_3—Na·Ca	1067.91	1065.37	-2.54
BS4	O_{2S+X}	HCO_3—Ca	1061.73	1059.8	-1.93
BS5	O_{2S+X}	$HCO_3 \cdot SO_4$—Ca	1064.47	1062.81	-1.66
BS6	O_{2S+X}	$HCO_3 \cdot SO_4$—Na·Ca	1061.96	1060.26	-1.7
G4	O_2+C_{3t}	HCO_3—Na·Ca	1191.86	1192.17	-0.31
G6	O_2+C_{3t}	$HCO_3 \cdot SO_4$—Na·Ca	1089.7	1033.56	-56.14

Table 2: Water quality and elevation table of each observation hole.

Water Temperature Discrimination

Table 3 shows changes in water temperature with depth of some hydrological boreholes in the area of Beixinyao Minefield. As depth increases, water temperature in the boreholes gradually increases. The temperature of the water outlet point was 11°. We know that the water temperature of the Carboniferous in Ningwu Shuonan coalfield generally exceeds 20°. Water temperatures at the water outlet point and in the Ordovician limestone water are nearly 10°: The water at the water outlet is not pure Ordovician limestone water, and the aquifer in the isothermal zone has a large recharge.

No.	Depth (m)	BS1 (°C)	BS2 (°C)	BS3 (°C)	BS4 (°C)	BS5 (°C)	BS6 (°C)	BS7 (°C)	BS8 (°C)
1	0	14.30	14.20	14.28	13.97	14.20	14.20	14.21	14.27
2	20	14.35	14.19	14.36	14.07	14.01	14.19	14.32	14.36
3	40	14.46	14.12	14.57	14.20	14.09	14.12	14.39	14.42
4	60	14.69	14.04	14.72	14.39	14.04	14.04	14.47	14.49
5	80	14.78	14.38	14.86	14.51	14.38	14.38	14.56	14.53
6	100	14.93	14.60	14.97	14.64	14.60	14.60	14.67	14.62
7	120	15.34	15.24	15.20	15.01	15.34	15.24	13.99	13.89
8	140	15.69	15.65	15.76	15.56	15.76	15.65	14.74	14.76
9	160	16.03	16.05	16.06	15.93	16.05	16.05	15.22	15.42
10	180	16.47	16.49	16.46	16.47	16.49	16.49	16.27	16.37

11	200	16.82	16.73	16.76	16.99	16.83	16.73	16.90	16.94
12	220	17.13	17.12	17.09	17.54	17.12	17.12	17.47	17.44
13	240	17.43	17.39	17.36	17.89	17.41	17.39	17.77	17.79
14	260	17.79	17.65	17.76	18.41	17.65	17.65	18.40	18.44
15	280	18.16	17.96	18.06	18.69	17.94	17.96	18.63	18.71
16	300	18.41	18.31	18.46	18.96	18.31	18.31	18.76	18.89
17	320	18.63	18.53	18.66	19.28	18.53	18.53	18.96	19.18
18	340	18.93	18.76	18.76	19.59	18.76	18.76	19.21	19.69
19	360	19.22	19.10	19.26	19.81	19.10	19.10	19.43	19.81
20	380	19.55	19.44	19.66	19.93	19.40	19.44	19.72	20.06
21	400	19.84	19.79	19.86	20.05	19.85	19.79	20.05	20.15
22	420	20.21	20.06	20.11	20.28	20.08	20.06	20.38	20.38
23	440	20.62	20.43	20.34	20.58	20.45	20.43	20.76	20.71
24	460	20.85	20.69	20.87	20.79	20.65	20.69	21.01	21.11
25	480	21.23	20.93	20.95	21.21	20.99	20.93	21.45	21.45
26	500	21.46	21.29	21.31	21.62	21.37	21.29	21.65	21.65

Table 3: Temperature measurements of each hydrological drilling hole.

Determination of Radioisotopes in Water Samples

In isotope hydrogeology, groundwater formed before 1953 is usually referred to as “paleowater” and groundwater formed after 1953 is referred to as “new water”. After 1963, due to reductions in nuclear testing, tritium concentrations also decreased. Accordingly, groundwater formed after 1963 is called “recent water” or “modern water”. Qualitative estimations of groundwater age are based on tritium content (mainland region) [16-18]. Shown as (Table 4).

Values	Groundwater age
< 0.8 TU	Ancient water and before 1953
0.8~4TU	Mixture of after 1963 and before 2010
5~15TU	Modern water less than 5-10 years

Table 4: Qualitative estimation of groundwater age using tritium content.

The 17 samples taken from each aquifer in Beixinyao Minefield were analyzed in the laboratory of the School of Environmental Science in the China University of Geosciences in Beijing, producing the results shown in Table 5.

Sample No.	Sampling sources	^{3}H（TU）	±（TU）
1	First mining face at 1000 m (C_3t)	7.3	0.3
2	Return shaft (C-P)	3.8	0.2
3	Return airway in south (P_1s)	5.7	0.2

4	Belt lane in south (C_3t)	3.5	0.1
5	BK16 well (C-P)	3.1	0.1
6	Return airway in south (P_1s)	1.5	0.1
7	Belt lane in south (C_3t)	3.5	0.1
8	Return shaft (C-P)	3.6	0.1
9	First mining face at 1000 m (C_3t)	3.6	0.1
10	Hui River	3.9	0.1
11	Shentou Spring	4.3	0.1
12	Belt lane in south (C_3t)	--	--
13	Return shaft (P)	3.2	0.1
14	BKS27 (C_3t)	3.0	0.1
15	BK16 well (O_2s)	2.6	0.1
16	BKS14 (O_2s)	2.8	0.1
17	BKS27 (O_2s)	--	--

Table 5: Content of tritium (^3H) at each sampling point.

From Table 5 and the histogram of tritium content in different samples Figure 5, it can be seen that the tritium content of the Huihe River water sample is 3.9 ± 0.21Tu, indicating that the mix of groundwater and surface water in this area is sub-modern water. The tritium content of Shentou Spring is higher than that of the Huihe River, indicating that Shentouquan has atmospheric precipitation recharge. The tritium content of the other 9 aquifer samples showed that the Shanxi mining group No. 1 in the first mining face had a large value of 7.3, indicating the presence of fresh water or tap water. This water is modern water, consistent with the afore-mentioned deuterium and oxygen analysis, and is allowed to have tap water mixed with it during processing. The tritium content of sample No. 3 in the Shihezi Formation of Huifeng Lane, South Wing is more than 5 Tu, corresponding to modern water; the remaining 7 samples have a tritium content of 1.5-4.3 Tu, corresponding to sub-modern water.

The ^{14}C isotope test of the foregoing 17 samples is also performed in the isotope liquid scintillator laboratory of the School of Environmental Science in the University of Geosciences in Beijing, using an ultra-low liquid scintillation spectrometer (Table 6). If the ^{14}C age is less than 1 ka, it can be treated as modern water.

Sample No.	Sampling sources	Percent of Modern Carbon (PMC %)	Errors (PMC %)	^{14}C Age （ka B.P.）	±
1	First mining face at 1000 m (C_3t)	72.2	1.5	2.69	0.17
2	Return shaft (C-P)	72.3	1.5	2.69	0.17
3	Return airway in south (P_1s)	75.9	1.5	2.28	0.17
4	Belt lane in south (C_3t)	75.6	1.5	2.32	0.17
5	BK16 well (C-P)	78	1.5	2.06	0.16
6	Return airway in south (P_1s)	75.9	1.7	2.28	0.19
7	Belt lane in south (C_3t)	73.7	1.7	2.52	0.19

8	Return shaft (C-P)	81.9	1.8	1.65	0.18
9	First mining face at 1000 m (C_3t)	73.4	1.7	2.55	0.19
10	Hui River	74.8	1.7	2.4	0.19
11	Shentou Spring	96	1.9	0.34	0.17
12	Belt lane in south (C_3t)	64.7	3.2	3.60	0.40
13	Return shaft (P)	72.4	3.3	2.67	0.38
14	BKS27 (C_3t)	66.4	3.2	3.38	0.40
15	BK16 well (O_2s)	77.8	3.5	2.07	0.37
16	BKS14 (O_2s)	--	--	--	--
17	BKS27 (O_2s)	--	--	--	--

Table 6: ^{14}C age table of aquifers at each sampling point.

According to Table 6 and the histogram of the ^{14}C age value of each sampling point, the groundwater age of Shentou Spring is 0.34 ka B.P., which corresponds to modern water, indicating that the water sample taken by Shentou Spring is surface water. The Huihe water sample represents the mixed water of groundwater and surface water in well fields and thus is sub-modern.

During the long-term pumping process, the ^{14}C age of the groundwater in the aquifer of the South Wing Belt Lane (Shanxi Formation) keeps increasing, and its age is very different from the ^{14}C age of the Taiyuan Formation aquifer groundwater collected during the same period, indicating that the groundwater is being replenished by old groundwater.

This indicates that there is a mixture of groundwater in the aquifers of the Taiyuan and Shanxi formations. The ^{14}C groundwater in the BKS27 Taiyuan Formation is older, indicating the presence of old groundwater of Ordovician aquifers. Differences in groundwater age between the BK16 (Shanxi and Taiyuan Formation) and BK16 (Ordovician) water samples within the margin of error are extremely small, further indicating a hydraulic connection between the Taiyuan Formation and the Ordovician aquifer.

In summary, there is a hydraulic connection between the Shihezi aquifer and the Cenozoic, and the Shanxi, Taiyuan, and Ordovician aquifers are mixed with one another. Moreover, water-conducting fault tectonic networks not only provide runoff channels and storage sites for groundwater in Ordovician limestone water and the Taiyuan and Shanxi formations, but are also the main controlling factors and prerequisites for runoff in various aquifers.

Trace Element Measurements of Water Samples

Geochemical studies of groundwater trace elements and isotopes in the well field have found that the Ordovician and Taiyuan Formation aquifers in the well field have high quality groundwater. It is initially determined that they have reached the standard for drinking natural mineral water, featuring high strontium (Sr) mineral water of great potential value.

Analysis of the laboratory testing results of 16 samples collected in 2018 and 2019 Table 7 revealed lower Li, Zn, Se, metasilicic acid, and free CO2 content than those specified in 'National Food Safety Standard Drinking Natural Mineral Water' (GB8537-2018). The local sampling lithium (Li) meets the standard's requirements, and the strontium (Sr) content of all samples meets the requirements of the specification (≥ 0.2mg/L), so water quality in this area has reached the limit for strontium mineral water.

	Li	Sr	Zn	Se	CO_2	TDS
International standard （≥） mg/L		0.2	0.2	0.01	250	1000
1 (C_3t)	0.0001	0.5689	0.0001	0.0001	60.43	335.09
2 (P)	0.0001	0.6201	0.0001	0.0001	91.37	333.14
3 (P_1s)	0.0001	0.872	0.0001	0.0057	89.61	351.39
4 (C_3t)	0.0001	1.2958	0.0001	0.0001	83.32	545.87
5 (C)	0.0001	2.9141	0.0001	0.003	118.16	413.0555
6 (P_1s)	0.0165	1.8263	0.0001	0.0001	104.44	390.8255
7 (C_3t)	0.0015	3.0112	0.0001	0.0001	100.15	273.923
8 (P)	0.0016	1.1739	0.0001	0.0001	75.53	327.262
9 (C_3t)	0.0012	2.1181	0.0001	0.0001	87.82	662.1875
10 (Hui River)	0.0125	3.39	0.0001	0.0001	97.54	198.3345
11 (Shentou Spring)	0.0022	0.786	0.0001	0.0001	73.21	500.5
12 (C_3t)	0.2804	0.5262	0.0021	na	17.6040	339.95
13 (P)	0.2766	0.2762	0.0057	na	17.6040	na
14 (P_1s)	0.0335	0.4602	0.0068	0.0033	na	634.4
15 (O_2s)	0.2822	0.5246	0.0123	na	79.2180	877.5
16 (C_3t)	0.3108	0.4987	0.0051	na	17.6040	248.10

Table 7: Table of groundwater limit indicators of Beixinyao.

Verification and Grouting of Thousands of Holes downhole

To allow smooth development of the three main roads in the south wing of Beixinyao Coal Mine and ensure safe production for the mine Figure 6, construction of directional water exploration boreholes in the three main roads in the south wing of Beixinyao Mine is needed to facilitate detection of faults for water gushing conditions, providing a strong basis for the next step in water treatment.

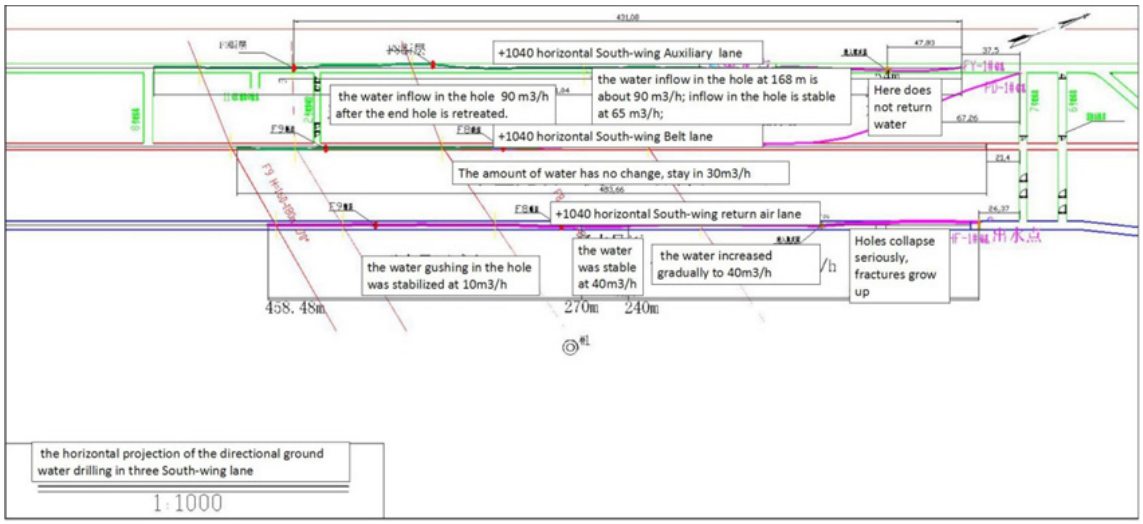

Figure 6: Horizontal projection of horizontal drilling in 7 kilometers.

Discussion

In this study, we investigated a case study in the Beixinyao Coal Mine to compare with several drilling data for the validation. In South-wing return Air Lane, there were two drilling holes: HF-1# and HF-4#. For HF-1#, the footage was 459 m and the Ordovician limestone was 102 m, while the faults F8 and F9 were found at 270 m and 416 m, respectively. There were seriously collapsed holes with abnormal return of water and slag occurred at 60-80 m. It is inferred that the fissures developed there. The water gushing in the hole of 80-240 m section increased gradually to 40 m^3/h from 30 m^3/h, and the surge began to decrease after 270 m. The final drilling hole was stabilized at l0 m^3/h. In comparison, for HF-4#, the footage was 210 m and the Ordovician limestone was 108 m. The water inflow (about 20 m^3/h) appeared at 42 m. It is inferred that the fissures were developed nearby. There is no obvious change in the water inflow in the final drilling hole (stable at about 20 m^3/h); and the final hole was stable at 45 m^3/h.

In South- wing Belt Lane, there was one drilling hole: PD-1#, in which the footage is 513 m, the Ordovician limestone is 67 m, while the faults F8 and F9 were found at 333 m and 448 m, respectively. The water inflow (about 30 m^3/h) appeared at 54m. It is inferred that the fissures were developed, but there is no obvious change in the water inflow in the final drilling hole (stable at about 30 m^3/h); and the final drilling hole was stable at 60 m^3/h [19-21].

In South-wing Auxiliary Lane, there was one drilling hole: FY-1#. The footage was 522 m and the Ordovician limestone is 48 m, while the faults F8 and F9 were found at 341 m and 431 m, respectively. The water inflow was appeared at 54 m. It is inferred that the fissures were developed. Till 120 m deep, it was gradually increased to 100 m^3/h; when stopped drilling, the water inflow in the drilling hole was stable at 40 m^3/h; while the drilling hole was deep to 168 m, the water inflow was about 90 m3/h, then dropped to be stable at 65 m^3/h, and slightly increased to be stable at 75 m^3/h; and finally the water [22,23]. In flow in the drilling at 90 m^3/h after the end hole was retreated.

Based on the construction situation for kilometer drilling, some new findings can be made:

1. The drilling water output of the three main lanes, from east to southwest wing back wind lane, south wing belt lane, and south wing auxiliary transport lane, increased, indicating that the source of recharge water came from the western Huihe River water diversion structural belt.
2. When the borehole passes through the F8 fault, rock is severely broken and water volume increases. After drilling is completed, water volume stayed steady, indicating that the F8 fault conducts water of certain water richness: When it passes through the F9 fault, borehole water volume is not obvious. The increase indicates poor conductivity of the F9 fault.
3. When grouting at the water outlet of the south wind wing of the east wing, the water outlet is completely stopped after grouting the Ordovician limestone, coal seam roof, and bottom sandstone aquifer. Accordingly, the presence of water outlet for the south wing auxiliary transportation road in the west will significantly reduce gushing, showing that the water outlets of the three roadways conduct water from northeast and northwest to the structure.

Conclusions

This study investigated and analyzed the water-inrush source of mining underground water in Beixinyao Coal Mine in Datong, Shanxi Province, China. Fieldwork featuring sample collection informs data analysis based on laboratory testing when seeking to investigate underground water inrush sources in coalmines and to accurately determine causes of water outflow in mining wells that feature water gushing, allowing to timely formulation of measures for effective controlling water damage and ensuring safe production, as at Beixinyao Coal Mine.

Certain conclusions may be drawn about similar conditions in other coalmines:

1. Based on multi-parameter measurement and analysis of water outlets and observation holes of Beixin Kiln, water discharge, quality, and temperature of outlets of the South Wing Backward Lane, South Wing Belt Lane, and South Wing Auxiliary Transport Lane are similar. Analysis of water, isotopes and trace elements shows strong correlation with structure.
2. The source of the water outlet is the replenishment of Huihe structural fault water from north to south. The Huihe structural fault water cuts the top, floor sandstone and Ordovician coal seam of Taiyuan Formation through the northeastward F8 fault, the northwestward nappe structure and the secondary structure and the Ordovician Limestone, recharging all fractured water aquifers and laterally recharging the middle and east of the minefield. Thus, prevention and control of coalmine water is focused on the northeast and northwest tectonic treatment of the flanks of the north-south structural water channel.
3. The north-south structural water in the west of the well field is strontium-rich mineral water. In preventing and controlling water in mines, the principles of coal and water coproduction should be combined to develop strontium-rich mineral water in coalmines, leading to potential local socioeconomic developments.

Author Contributions

Conceptualization, Y.G. and J.G. methodology, Y.G.; software, J.G.; validation, Y.G., J.C. and Y.Z.; formal analysis, Y.C.; investigation, Y.G.; resources, J.Y.; data curation, J.G.; writing-original draft preparation, Y.G.; writing-review and editing, Y.Z.; visualization, J.G.; supervision, Y.Z.; project administration, J.Y.; funding acquisition, Y.G.

Funding

This research was funded by the National Natural Science Foundation (U1901215), the Natural Scientific Foundation of Jiangsu Province (BK20181413), and the Marine Special Program of Jiangsu Province in China (JSZRHYKJ202007).

Acknowledgments

Water samples were analyzed by the laboratory of the School of Environmental Science in the China University of Geosciences in Beijing, China. We also thank the support from the National Natural Science Foundation (U1901215), the Natural Scientific Foundation of Jiangsu Province (BK20181413), and the Marine Special Program of Jiangsu Province in China (JSZRHYKJ202007).

References

1. Du P (1964) Datong coalfield regional structures and their relationship to other structures. Geological Review 22: 259-266.
2. Fan EP, Yang ZW, Gao YP, Cheng YH, Zhao J (2018) Northern structural features and their coal controlling role. Coal Geology and Exploration 4: 8-16.
3. Guo WZ, Cheng YH, Gao YP (2015) Datong coalfield structural features and coal boundary in Taiyuan formation. Coal Geology and Exploration 043: 1-7.
4. He S (2006) Coal seam storage law of Pingshuo mining area in Ningwu coalfield, Shanxi Province, China. Journal of Shanxi College of Coal Management 3: 123-124.
5. Li ZH, Dong SW, Qu HJ (2013) Geo-chemistrical features and geological significance of Jurassic clastic rocks in Ningwu-Jingle basin. Geological Review 59: 637-655.
6. Li Y (2007) Detailed surveying for the main factors of coal depth change in southern Shuozhou No.4 coal seam. China Coal Geology 19: 19-21.
7. Tian WG, Tang DZ, Sun B (2010) Southern coal seam gas concentration main factors. Natural Gas Industry 30: 22-25.
8. Zhou AC (2010) Geological Research on Late Paleozoic Coal Basin in Datong Coalfield; Coal Technology Press, Beijing pp. 15-48.
9. Zhou XG (2015) Ningwu basin structural evolution and its controlling to storage of coal seam gas. Unpublished master's thesis, China University of Mining and Technology, Xuzhou.
10. Cai J, Zhang Y, Li Y, Liang XS, Jiang T (2017) Analyzing the Characteristics of Soil Moisture Using GLDAS Data: A Case Study in Eastern China. Applied Sciences 7: 566.
11. Huang RH, Sun FY (1994) Impacts of Thermal State and the Convective Activities in the Tropical Western Warm Pool on the Summer Climate Anomalies in East China. Scientia Atmospherica Sinica 18: 141-151.
12. Ji C, Zhang Y, Cheng Q, Li Y, Jiang T, et al. (2019) Analyzing the variation of the precipitation of coastal areas of eastern China and its association with sea surface temperature (SST) of other seas. Atmospheric Research, 219: 114-122.
13. Zhang Y, Huang Z, Fu D, Tsou JY, Jiang T, et al. (2018) Monitoring of chlorophyll-a and sea surface silicate concentrations in south part of Cheju island in the East China sea using MODIS data. International Journal of Applied Earth Observation and Geoinformation 67: 173-178.
14. Ji C, Zhang Y, Cheng Q, Tsou JY, Jiang T, et al. (2018) Evaluating the impact of sea surface temperature (SST) on spatial distribution of chlorophyll-a concentration in the East China Sea. International Journal of Applied Earth Observation and Geoinformation 68: 252-161.
15. Ma ZG, Wei HL, Fu ZB (2000) Relationship between Regional Soil Moisture Variation and Climatic Variablity over East China. Acta Meteorologica Sinica 58: 284-286.
16. Rodell M, Houser PR, Jambor U, Gottschalck J, Mitchell K, et al. (2004) The global land data assimilation system. Bulletin of the American Meteorological Society 85: 381-394.
17. Elsner J (2006) Evidence in support of the climate change-Atlantic hurricane hypothesis. Geophysical Research Letters 33: L16705.
18. Salvucci GD, Saleem JA, Kaufmann R (2002) Investigating soil moisture feedbacks on precipitation with tests of Granger causality. Advances in Water Resources 25: 1305-1312.
19. Su H (2015) Causality Analysis between Precipitation and Soil Moisture and Precipitation Prediction.
20. Liang XS (2014) Unraveling the cause-effect relation between time series. Physical Review E 90: 052150.
21. Chen LT, Wu RG (1998) The Joint Effects of SST Anomalies over Different Pacific Regions on Summer Rain belt Patterns in Eastern China. Scientia Atmospherica Sinica 22: 718-726.
22. Huang RH, Sun FY (1994) Impacts of Thermal State and the Convective Activities in the Tropical Western Warm Pool on the Summer Climate Anomalies in East China. Scientia Atmospherica Sinica 18: 141-151.
23. Chen LT (1988) Zonal anomaly of sea surface temperature in the tropical Indo-Pacific Ocean and its effect on summer Asia monsoon. Chinese Journal of Atmospheric Sciences 12: 142-148.